

DEFINITIVE IDENTIFICATION OF THE TRANSITION BETWEEN
SMALL- TO LARGE-SCALE CLUSTERING FOR LYMAN BREAK GALAXIES¹

MASAMI OUCHI ^{2,3}, TAKASHI HAMANA ⁴, KAZUHIRO SHIMASAKU ⁵, TORU YAMADA ⁴,
MASAYUKI AKIYAMA ⁶, NOBUNARI KASHIKAWA ⁴, MAKIKO YOSHIDA ⁵, KENTARO AOKI ⁶,
MASANORI IYE ⁴, TOMOKI SAITO ⁵, TOSHIYUKI SASAKI ⁶,
CHRIS SIMPSON ⁷, AND MICHITOSHI YOSHIDA ⁸

Submitted to ApJL

ABSTRACT

We report angular correlation function (ACF) of Lyman Break Galaxies (LBGs) with unprecedented statistical quality from a sample of 16,920 galaxies at $z = 4$ detected in the 1 deg^2 field of the Subaru/XMM-Newton Deep Field. The ACF significantly departs from a power law, and shows an excess on small scale. Particularly, the ACF of LBGs with $i' < 27.5$ have a clear break between the small and large-scale regimes at the angular separation of $\simeq 7''$ whose projected length corresponds to the virial radius of dark halos with a mass of $10^{11-12} M_\odot$, indicating multiple LBGs residing in a single dark halo. Both on small ($2'' < \theta < 3''$) and large ($40'' < \theta < 400''$) scales, clustering amplitudes monotonically increase with luminosity for the magnitude range of $i = 24.5 - 27.5$, and the small-scale clustering shows a stronger luminosity dependence than the large-scale clustering. The small-scale bias reaches $b \simeq 10 - 50$, and the outskirts of small-scale excess extend to a larger angular separation for brighter LBGs. The ACF and number density of LBGs are reasonably reproduced by a halo model in the framework of the halo occupation distribution of the Cold Dark Matter model.

Subject headings: large-scale structure of universe — galaxies: formation — galaxies: high-redshift

1. INTRODUCTION

Recently, there has been great progress in the observations of large-scale structures at high redshifts. Strong clustering has been found in the two-point angular correlation function (ACF) of Lyman break galaxies (LBGs) at $z = 3 - 5$, (e.g. Giavalisco & Dickinson 2001; Ouchi et al. 2001; Foucaud et al. 2003; Adelberger et al. 2003; Ouchi et al. 2004b; Hildebrandt et al. 2004; Allen et al. 2005), red galaxies at $z = 3$ (Daddi et al. 2003), and Ly α emitters (LAEs; Ouchi et al. 2003; Shimasaku et al. 2004) at $z = 5$. Even at $z = 6$, there is a piece of evidence for filamentary large-scale (100 Mpc-scale) structures of LAEs whose rms fluctuation is comparable to those of present-day galaxies (Ouchi et al. 2005). The strong clustering indicates that the distribution of high- z galaxies is fairly inhomogeneous and highly biased in comparison with the matter distribution predicted by the Cold Dark Matter (CDM) model. The estimated bias is in the range of $b \simeq 2 - 8$, depending both on luminosity/type and redshift of galaxies. However, the shape of the ACF for high- z galaxies is not well constrained; i.e., Ouchi et al. (2001) reported the significant excess of ACFs at $\theta < 5''$, while Porciani & Giavalisco (2002) found that the ACF at $10'' \lesssim \theta \lesssim 30''$ becomes small.

¹ Based on data collected at Subaru Telescope, which is operated by the National Astronomical Observatory of Japan.

² Space Telescope Science Institute, 3700 San Martin Drive, Baltimore, MD 21218, USA; ouchi@stsci.edu.

³ Hubble Fellow

⁴ National Astronomical Observatory, Tokyo 181-8588, Japan

⁵ Department of Astronomy, School of Science, University of Tokyo, Tokyo 113-0033, Japan

⁶ Subaru Telescope, National Astronomical Observatory, 650 N.A'ohoku Place, Hilo, HI 96720, USA

⁷ Department of Physics, University of Durham, South Road, Durham DH1 3LE, UK

⁸ Okayama Astrophysical Observatory, National Astronomical Observatory, Kamogata, Okayama 719-0232, Japan

In the local universe, the correlation function shows a departure from a power law (e.g. Connolly et al. 2002; Hawkins et al. 2003; Zehavi et al. 2004). The departure is reproduced in the framework of the halo occupation distribution (HOD) and the related halo models in the standard CDM cosmology (van den Bosch et al. 2003; Magliocchetti & Porciani 2003; Zehavi et al. 2004; Benson et al. 2001; Berlind et al. 2003), and explained by two sources contributing to the correlation function; one for galaxy pairs residing in the same halo (1-halo term) and the other for galaxies hosted by different halos (2-halo term; see, e.g., Zehavi et al. 2004). The HOD has been applied to clustering of high- z galaxies as well as local galaxies (Bullock et al. 2002; Moustakas & Somerville 2002; Hamana et al. 2004). However, parameters of the models have not been constrained with similar accuracy as at low redshifts, because the sample size and surveyed area are still relatively small, i.e., $0.01 - 0.1 \text{ deg}^2$ and $100 - 2000$, respectively.

In this paper, we present ACF of $z = 4$ LBGs with unprecedented statistical quality, on the basis of large high- z galaxy sample (16,920 LBGs) obtained by the wide-field (1 deg^2) survey in Subaru/XMM-Newton Deep Field (SXDF; Sekiguchi et al. 2004). Throughout this paper, magnitudes are in the AB system, and we adopt $H_0 = 70h_70 \text{ km s}^{-1} \text{ Mpc}^{-1}$ and $[\Omega_m, \Omega_\Lambda, n, \sigma_8] = [0.3, 0.7, 1.0, 0.9]$. To facilitate comparison with previous results, we express r_0 using h_{100} , where h_{100} is the Hubble constant in units of $100 \text{ km s}^{-1} \text{ Mpc}^{-1}$.

2. DATA AND SAMPLE

We carried out deep optical broad-band imaging with Subaru/Suprime-Cam (Miyazaki et al. 2002) in the 1 deg^2 sky of the SXDF. Our broad-band (B, V, R, i' , and z') images reach $B \simeq 28.3, V \simeq 27.3, R \simeq 27.6, i' \simeq 27.5$, and $z' \simeq 26.5$ with a $2''$ -diameter circular aperture at the

3σ level (Furusawa et al. in preparation; see Sekiguchi et al. 2004). Typical seeing sizes (FWHM) of these images are $0''.8$. We use the i' -band selected source catalog of the SXDS Ver1.0 which is composed of 0.7 million objects with $i' < 27.5$. We select LBGs at $z = 4.0 \pm 0.5$ on the basis of the color criteria of Ouchi et al. (2004a), i.e., $B - R > 1.2$, $R - i' < 0.7$, and $B - R > 1.6(R - i') + 1.9$, which were determined with the results of spectroscopy and Monte-Carlo simulations. Twenty thousand LBG candidates satisfy the color criteria. We visually inspect all the candidates and mask areas contaminated with halos of bright stars and CCD blooming. Our final catalog includes 16,920 LBGs in a 1.00 deg^2 area. Figure 1 shows the sky distribution of our LBGs. We summarize our LBG samples in Table 1. Our spectroscopic follow-up observations show that 60 out of 63 identified candidates are real LBGs at $z = 3.5 - 4.5$; i.e., 17 out of 17 and 43 out of 46 are LBGs in the SXDF (Akiyama M. in preparation) and in the Subaru Deep Field, respectively, where the latter LBG sample is made with the same color criteria as ours (Yoshida 2005). Thus, the contamination rate of our LBG sample is roughly estimated to be $(63 - 60)/63 = 5\%$.

3. RESULTS AND DISCUSSION

3.1. Definitive Identification of the Transition between Small and Large-Scale Clustering

We derive the ACF, $\omega(\theta)$, by the formula of Landy & Szalay (1993) with random samples composed of 200,000 sources, and estimate bootstrap errors (Ling et al. 1986). Since clustering properties of our 5% sample contaminants are not clear, we do not apply the contamination correction for $\omega(\theta)$ with the assumption of the random distribution for contaminants (c.f. Ouchi et al. 2004b). However, this correction changes $\omega(\theta)$ and bias only by 10% or less. Figure 2 presents the ACF of LBGs (top panel), residuals of a power-law fit (middle panel), and galaxy-dark matter bias (bottom panel) defined as $b(\theta) \equiv \sqrt{\omega(\theta)/\omega_{\text{dm}}(\theta)}$, where $\omega_{\text{dm}}(\theta)$ is the ACF predicted by the non-linear model of Peacock & Dodds (1996). In the top and middle panels of Figure 2 the ACF of LBGs shows a significant excess on small scale, and indicates that a power law, $A_\omega \theta^{-\beta}$, does not fit the data. This is the definitive identification of the departure from a power law for the ACF of LBGs at $z = 4$. It should be noted that we have visually inspected all close-pairs of LBGs and have confirmed that they are not false detections. Moreover, a very recent study by Lee et al. (2005) also finds a similar small-scale excess for $z = 4 - 5$ LBGs in a sample obtained by HST/ACS-GOODS.

Comparing our ACF with the one of dark matter, we find that the small-scale excess extends up to $\simeq 7''$, i.e. $0.24h_{70}^{-1} \text{ Mpc}$, which is comparable to the virial radius, r_{200} , of dark halos with a mass of $10^{11-12} M_\odot$ (see the ticks in the top panel of Figure 2), where r_{200} is a sphere of radius within which the mean enclosed density is 200 times the mean cosmic value (Mo & White 2002). Interestingly, the large-scale average bias at $40'' < \theta < 400''$ is estimated to be 2.9 ± 0.2 which is also comparable to the linear bias of dark halos with a mass of $10^{11-12} M_\odot$ ($b = 2.2 - 3.5$) predicted by the analytic model of CDM (Sheth & Tormen 1999; see the ticks in the bottom panel of Figure 2). This coincidence of the dark-halo mass

strongly supports that typical $z = 4$ LBGs reside in dark halos with a mass of $10^{11-12} M_\odot$. Moreover, these pieces of evidence suggest that multiple LBGs occupy a single dark halo, which can be modeled with the HOD. The middle panel of Figure 2 also plots residuals of a power-law fit for local galaxies (Zehavi et al. 2004), which is comparable to those of $z = 4$ LBGs on large scale, but significantly larger than LBGs on intermediate scale ($0.2 - 1.0 \text{ Mpc}$) corresponding to the radius of $10^{12-14} M_\odot$ dark halos. According to the halo mass function (e.g. Sheth & Tormen 1999), the ratio of galaxy-sized halos ($\sim 10^{10-12} M_\odot$) to group/cluster-sized halos ($\sim 10^{12-14} M_\odot$) is about 10 times higher in number density at $z = 4$ than at $z = 0$. This relative deficit of group/cluster-sized halos at high redshifts would be the cause of the clearer break between small and large-scale ACFs at $z = 4$ than $z = 0$.

The small-scale bias of LBGs shown in the bottom panel of Figure 2 is particularly interesting. In the present-day universe, late-type galaxies are antibiased on small scale, while early-type galaxies are positively biased (van den Bosch et al. 2003). This is often interpreted as due to the environmental effects of galaxy distribution (e.g. Dressler 1980). Although LBGs are star-forming galaxies classified as the spectral type similar to that of late-type galaxies, $z = 4$ LBGs are positively and even very strongly biased on small scale. The reason for this difference is not clear, but it would indicate that multiple star-forming galaxies are more likely hosted by a single dark halo at $z = 4$ than $z = 0$, thus suggesting that galaxy formation efficiency (i.e. star-formation rates per mass) may be very high in dark halos at high redshifts.

3.2. Luminosity Dependence of Small and Large Scale Clustering

We calculate $\omega(\theta)$ and b for six subsamples with limiting magnitudes of $i' < 24.5, 25.0, 25.5, 26.0, 26.5$, and 27.0 (Figure 3). The small- ($2'' < \theta < 3''$; $0.05 - 0.07h_{100}^{-1} \text{ Mpc}$) and large- ($40'' < \theta < 400''$; $1 - 10h_{100}^{-1} \text{ Mpc}$) scale biases for each subsample are shown in Figure 4. Although luminosity segregation of large-scale clustering is reported for $z = 4$ LBGs (Ouchi et al. 2004a; Allen et al. 2005; Lee et al. 2005), we find in Figures 3 and 4 that ACFs and biases monotonically decrease from $i' < 24.5$ to $i' < 27.5$ on small scale as well as large scale. Interestingly, Figure 4 shows that the small-scale bias has a stronger dependence on luminosity ($b \simeq 10 - 50$) than the large-scale bias ($b \simeq 3 - 4$), and the bottom panels of Figure 3 indicate that outskirts of small-scale excess extend to $\theta \sim 10''$ for bright ($i' < 24.5 - 25.5$) LBGs. All the features of luminosity dependence suggest that bright LBGs reside in more massive dark halos, since massive dark halos have not only a high large-scale bias, but also a high small-scale bias (i.e. high probability of pair galaxies in a massive halo) and an extended outskirt of bias due to a large halo size.

Although the ACFs depart from a power law, we approximate the ACFs with a power law, in order to compare our results with the previous clustering results. We fit the ACF over $1 - 1000''$ with $\omega(\theta) = A_\omega(\theta^{-\beta} - \text{IC}/A_\omega)$, where IC is the integral constraint (Groth & Peebles 1977). The bottom panel of Figure 4 presents the best-fit slopes, β , as a function of magnitude. The slopes, β , be-

come flatter at faint magnitudes (see also Kashikawa et al. 2005). This luminosity dependence of β is explained by the strong luminosity dependence of small-scale clustering as discussed above. Then we calculate the Limber integral equation and estimate the correlation lengths, r_0 , which is the normalization of the spatial two-point correlation function, $\xi = (r/r_0)^{-\gamma}$, where $\gamma = \beta + 1$ (see Ouchi et al. 2004b for these calculations). We apply the redshift distribution function used in Ouchi et al. (2004b). Table 1 presents the best-fit parameters, A_ω , β , together with r_0 . These r_0 are consistent with those obtained by Ouchi et al. (2004b) as well as by Hildebrandt et al. (2004) and Kashikawa et al. (2005). However, our results are not consistent with those of small-sky surveys in HDF, if we assume that ACF does not significantly evolve between $z = 3$ and 4 (Ouchi et al. 2004b). For examples, Giavalisco & Dickinson (2001) find a small correlation length of $r_0 = 1.0_{-0.7}^{+0.8} h_{100}^{-1}$ Mpc for $z = 3$ LBGs, while we find a significantly larger value, $r_0 = 3.9_{-0.2}^{+0.2} h_{100}^{-1}$ Mpc, for our $i' < 27.5$ LBGs whose number density is comparable to that of Giavalisco & Dickinson (2001) ($1 \times 10^{-2} h_{70}^3$ Mpc $^{-3}$). We restrict our power-law fitting to the same narrow range as Giavalisco & Dickinson (2001) ($1'' \lesssim \theta \lesssim 20''$), and then we obtain the consistent results within a 2σ level, i.e. $r_0 = 1.1 \pm 0.2 h_{100}^{-1}$ Mpc and $\beta = 1.9$, which are due to the fitting only to the small-scale excess of the ACF (see also Kravtsov et al. 2004). Similarly, the correlation length of red galaxies in HDF-S ($r_0 = 8 h_{100}^{-1}$ Mpc; Daddi et al. 2003) is probably overestimated by the extrapolation from a bump of small-scale ACF with a relatively flat slope of $\beta = 0.8$, which is also

claimed by the model of Zheng (2004).

3.3. Comparison with a Halo Model

We fit the halo model of Hamana et al. (2004) to the ACF and number density of LBGs (Table 1). This model predicts number density and ACF contributed by 1-halo and 2-halo terms in the framework of the HOD of the CDM model. The best-fit models are shown in Figure 3. These models reasonably account for the overall shape of our ACFs, i.e., the small-scale excess as well as the large-scale clustering (see also Lee et al. 2005), although there remain large residuals (e.g. reduced $\chi^2 = 3.4$ for $i' < 27.5$ LBGs). These residuals may imply that we need more precise modeling for the ACFs of our LBGs. Table 1 summarizes the average number of LBGs in a halo, $\langle N_g \rangle$ and the average masses of the halo, $\langle M_h \rangle$ (see Hamana et al. 2004 for definition) for the best-fit models. The average mass of hosting halos monotonically decreases from $2 \times 10^{12} h_{70}^{-1} M_\odot$ ($i' < 24.5$) to $5 \times 10^{11} h_{70}^{-1} M_\odot$ ($i' < 27.5$). The average number of LBGs in one halo is less than unity, $\langle N_g \rangle \simeq 0.2 - 0.7$, while the model ACF in Figure 3 shows a significant 1-halo term produced by multiple LBGs in one halo. This implies that majority of halos with an average mass have no LBG and only some of these halos host one or multiple LBG(s). A more detailed discussion about model fitting will be presented in our forthcoming paper.

We thank M. Fall, M. Giavalisco, K. Lee, S. Okamura, and Z. Zheng for helpful comments and discussion.

REFERENCES

- Adelberger, K. L., Steidel, C. C., Shapley, A. E., & Pettini, M. 2003, ApJ, 584, 45
- Allen, P. D., Moustakas, L. A., Dalton, G., MacDonald, E., Blake, C., Clewley, L., Heymans, C., & Wegner, G. 2005, MNRAS, 523
- Arnouts, S., et al. 2002, MNRAS, 329, 355
- Bullock, J. S., Wechsler, R. H., & Somerville, R. S. 2002, MNRAS, 329, 246
- Benson, A. J., Frenk, C. S., Baugh, C. M., Cole, S., & Lacey, C. G. 2001, MNRAS, 327, 1041
- Berlind, A. A., et al. 2003, ApJ, 593, 1
- Connolly, A. J., et al. 2002, ApJ, 579, 42
- Daddi, E., et al. 2003, ApJ, 588, 50
- Dressler, A. 1980, ApJ, 236, 351
- Foucaud, S., McCracken, H. J., Le Fèvre, O., Arnouts, S., Brodwin, M., Lilly, S. J., Crampton, D., & Mellier, Y. 2003, A&A, 409, 835
- Giavalisco, M. & Dickinson, M. 2001, ApJ, 550, 177
- Giavalisco, M. 2005, "Wide-Field Imaging from Space", Berkeley, May 16-18 2004, Eds. Tim McKay, Andy Fruchter, and Eric Linder. Elsevier, in press
- Groth, E. J. & Peebles, P. J. E. 1977, ApJ, 217, 385
- Hamana, T., Ouchi, M., Shimasaku, K., Kayo, I., & Suto, Y. 2004, MNRAS, 347, 813
- Hawkins, E., et al. 2003, MNRAS, 346, 78
- Hildebrandt, H., et al. 2004, ArXiv Astrophysics e-prints, arXiv:astro-ph/0412375
- Kashikawa, N. et al. 2005, submitted to ApJ
- Kravtsov, A. V., Berlind, A. A., Wechsler, R. H., Klypin, A. A., Gottlöber, S., Allgood, B., & Primack, J. R. 2004, ApJ, 609, 35
- Landy, S. D., & Szalay, A. S. 1993, ApJ, 412, 64
- Lee, K. et al. 2005, submitted to ApJ
- Ling, E. N., Barrow, J. D., & Frenk, C. S. 1986, MNRAS, 223, 21P
- Magliocchetti, M., & Porciani, C. 2003, MNRAS, 346, 186
- Miyazaki, S. et al. 2002, PASJ, 54, 833
- Mo, H. J. & White, S. D. M. 2002, MNRAS, 336, 112
- Moustakas, L. A., & Somerville, R. S. 2002, ApJ, 577, 1 2002, MNRAS, 332, 827
- Ouchi, M. et al. 2001, ApJ, 558, L83
- Ouchi, M. et al. 2003, ApJ, 582, 60
- Ouchi, M., et al. 2004a, ApJ, 611, 660
- Ouchi, M., et al. 2004b, ApJ, 611, 685
- Ouchi, M., et al. 2005, ApJ, 620, L1
- Peacock, J. A., & Dodds, S. J. 1996, MNRAS, 280, L19
- Porciani, C., & Giavalisco, M. 2002, ApJ, 565, 24
- Sekiguchi, K. et al. 2004, Astrophysics and Space Science Library, 301, 169
- Sheth, R. K. & Tormen, G. 1999, MNRAS, 308, 119
- Shimasaku, K., et al. 2004, ApJ, 605, L93
- van den Bosch, F. C., Yang, X., & Mo, H. J. 2003, MNRAS, 340, 771
- Yoshida, M. 2005, Master Thesis, University of Tokyo
- Zehavi, I., et al. 2004, ApJ, 608, 16
- Zheng, Z. 2004, ApJ, 610, 61

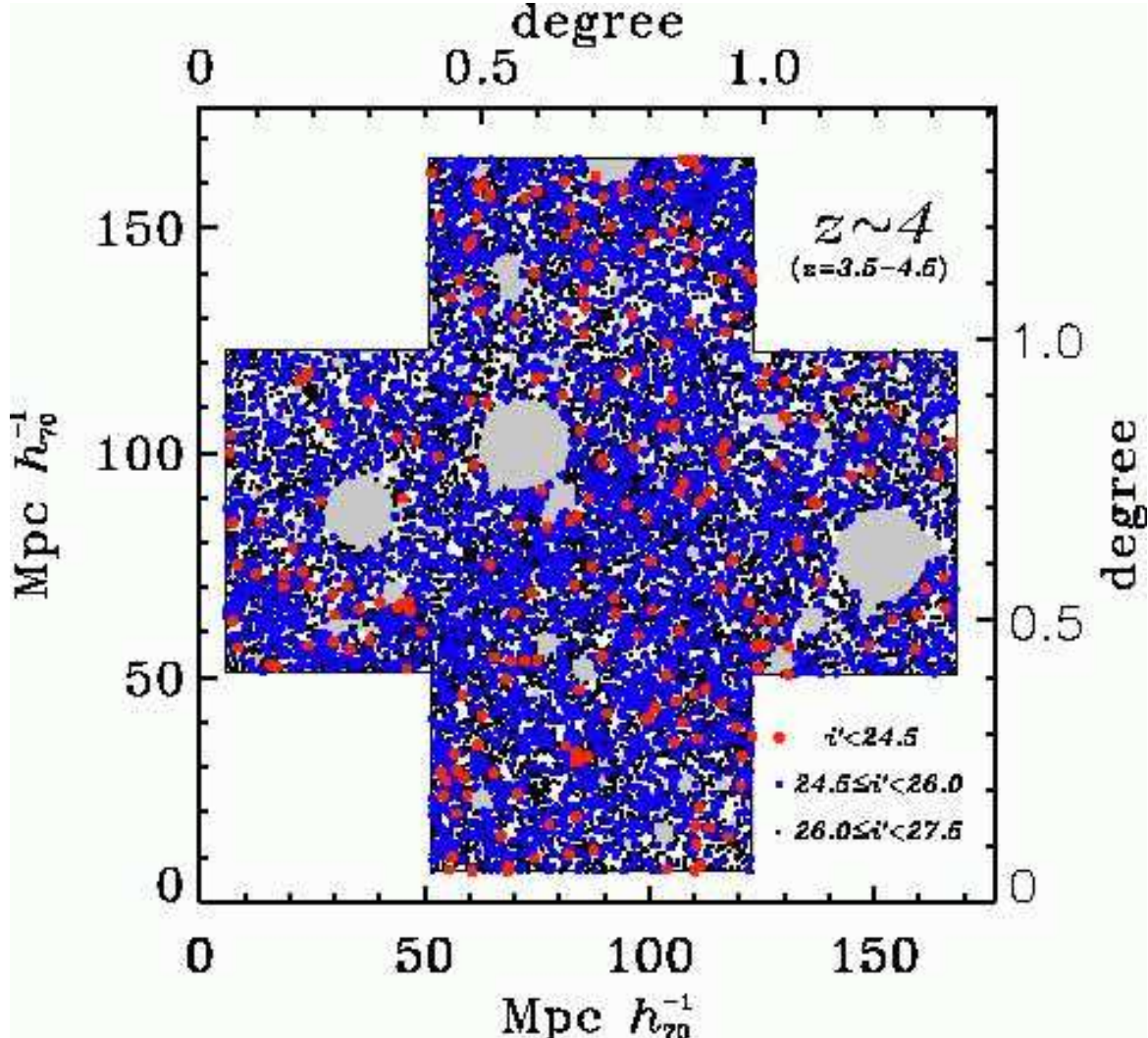


FIG. 1.— The distribution of LBGs at $z = 4.0 \pm 0.5$ in the SXDF. The red, blue, and black points denote the positions of the LBGs with $i' < 24.5$ (bright), $24.5 \leq i' < 26.0$ (intermediate), and $26.0 \leq i' < 27.5$ (faint), respectively. The gray areas present masked regions where we did not use for our analysis. The scale on the map is marked in both degrees and (comoving) megaparsecs for projected distance at $z = 4.0$. **This figure is degraded. This paper with the original figure can be downloaded from http://www-int.stsci.edu/~ouchi/work/astroph/sxds_z4LBG/ouchi_highres.pdf**

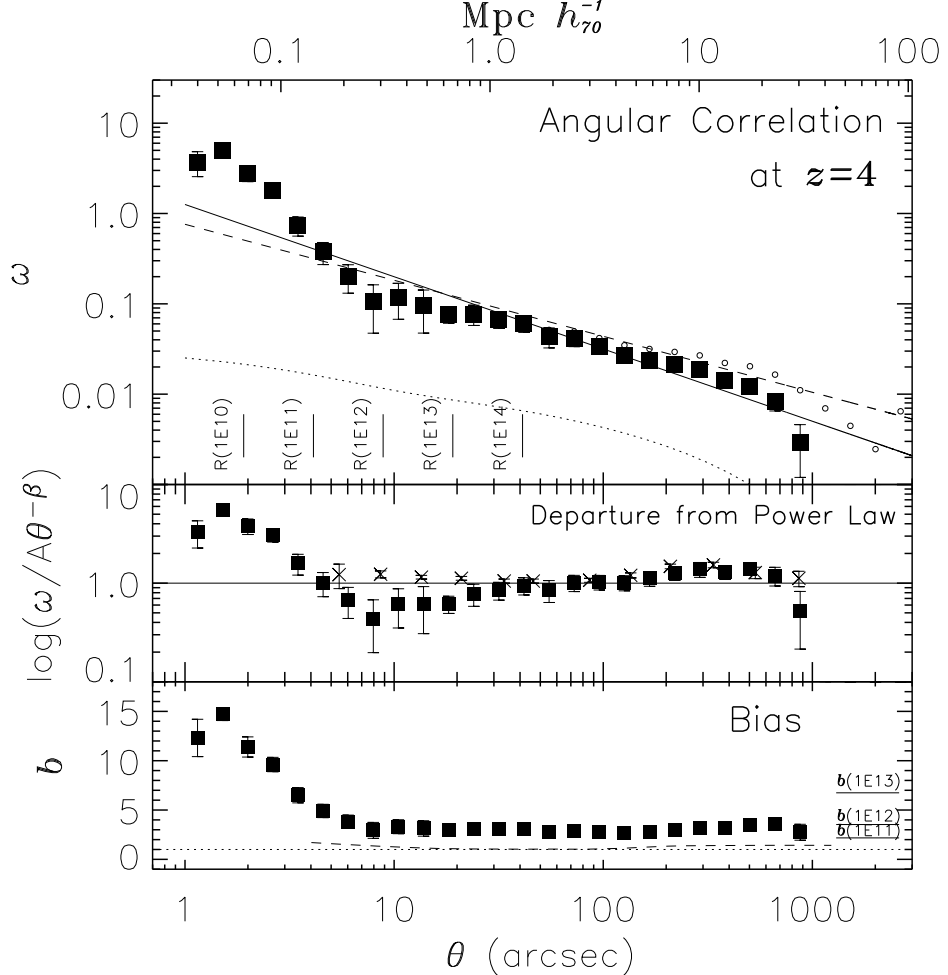


FIG. 2.— *Top* : The ACF, $\omega(\theta)$, of LBGs. The squares and error bars indicate the ACF and 1σ bootstrap errors of LBGs. The solid line is the best-fit power law ($A_\omega \theta^{-\beta}$; reduced $\chi^2 = 7.4$) for $1'' - 1000''$. The open circles are the ACF with IC correction under the assumption of the conventional power-law approximation, and the dashed lines are the best-fit power law for these open circles. The dotted curve is the ACF of dark matter predicted by the non-linear model of Peacock & Dodds (1996). The scale on the top axis denotes the projected distance in comoving megaparsecs at $z = 4.0$. The ticks labeled with $R(1E10)$, $R(1E11)$, $R(1E12)$, $R(1E13)$, and $R(1E14)$ correspond to the predicted virial radii of dark halos, r_{200} , with a mass of 1×10^{10} , 10^{11} , 10^{12} , 10^{13} , and $10^{14} h_{70}^{-1} M_\odot$, respectively. *Middle* : The ratios of the ACF to the best-fit power law for our LBGs (squares), together with those for local galaxies (crosses; Zehavi et al. 2004). *Bottom* : The galaxy-dark matter bias, b , of LBGs as a function of separation. The dashed curve presents bias of local galaxies (Zehavi et al. 2004). The ticks with $b(1E11)$, $b(1E12)$, and $b(1E13)$ show linear biases of dark halos with a mass of 1×10^{11} , 10^{12} , and $10^{13} h_{70}^{-1} M_\odot$, respectively, predicted by the analytic CDM model of Sheth & Tormen (1999).

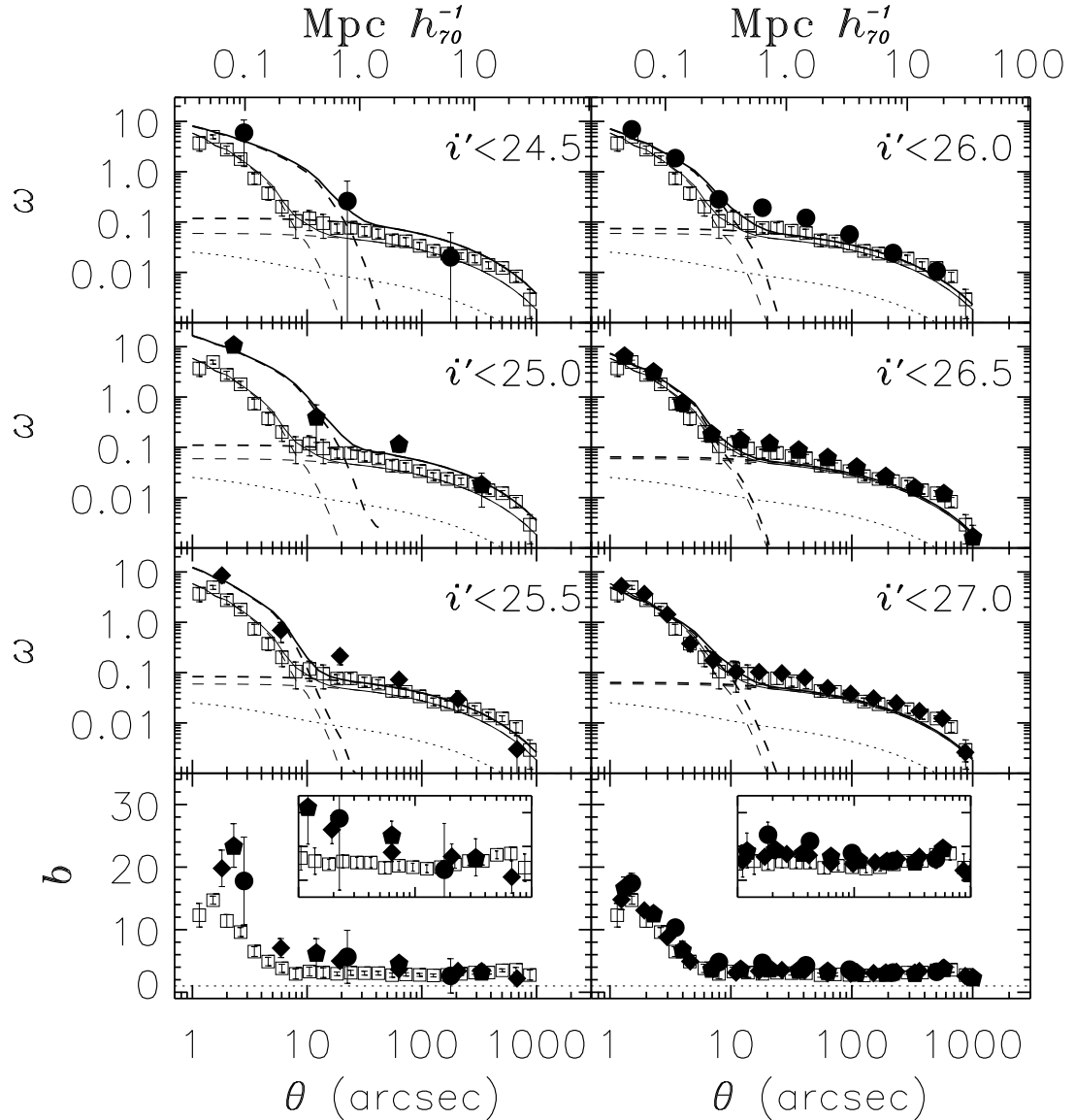


FIG. 3.— The ACFs of magnitude-limited subsamples of LBGs at $z = 4.0$. In the top to third-top panels, the filled symbols are the ACFs of our LBGs with the limiting magnitude indicated in the legend. Each of these panels shows the ACF of $i' < 27.5$ LBGs with open squares. The dotted curves are the ACF of dark matter predicted by the non-linear model of Peacock & Dodds (1996). The thick solid and dashed lines indicate the best-fit ACFs of the halo model and the breakdown of 1-halo and 2-halo terms for each subsample, while the thin lines are for $i' < 27.5$ LBGs. In the bottom panels, biases of LBGs for the each magnitude-limited subsample are presented with the filled symbols which correspond to those marks found in the top to third-top panels. The open squares are biases of LBGs with $i' < 27.5$. The plots of large-scale biases are magnified in the inserted boxes.

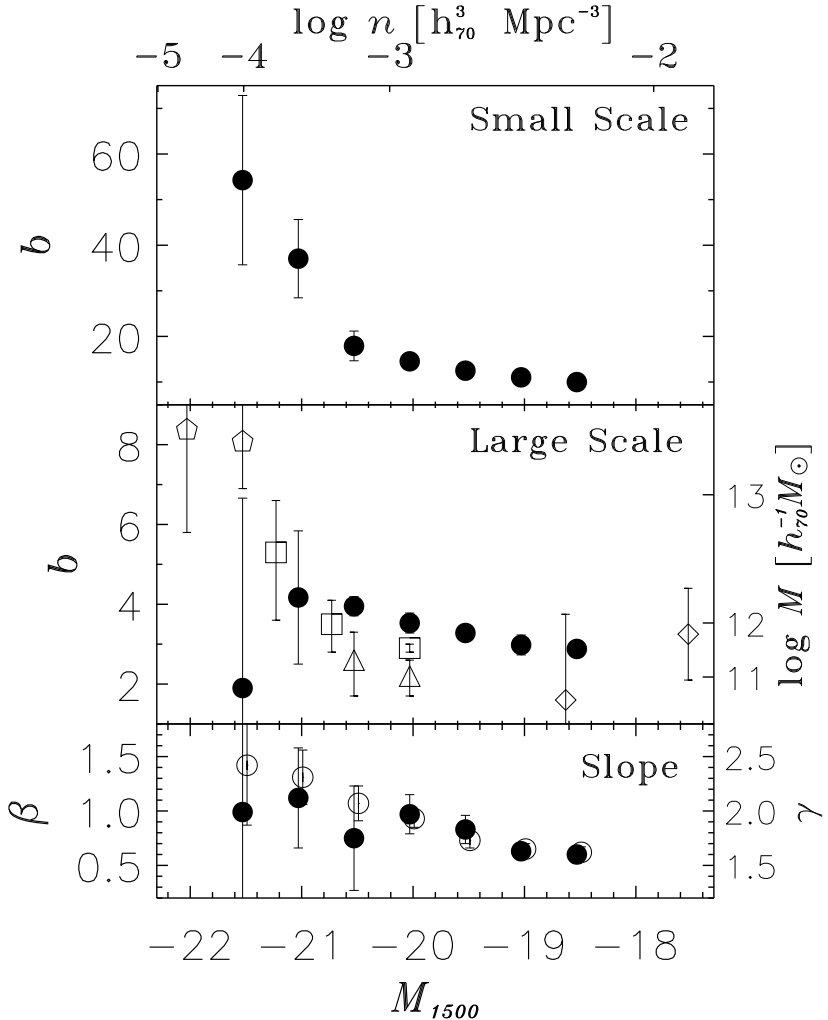


FIG. 4.— Bias and slope of $z = 4$ LBGs as a function of limiting-absolute magnitude calculated from $i' - M_{1500} = 46.0$. Top and middle panels present bias of small-scale ($2'' < \theta < 3''$) and large-scale ($40'' < \theta < 400''$) clustering. Filled circles plot for our LBGs, whose bias is directly measured from the ACFs. Open pentagons, squares, triangles, and diamonds present the large-scale ($\simeq 8h_{100}^{-1}$) bias estimated from the conventional power-law fit by Allen et al. (2005); Ouchi et al. (2004b, 2001); Arnouts et al. (2002). In the middle panel, the right-hand vertical scale means mass of dark halos corresponding to the linear bias (Sheth & Tormen 1999). The upper abscissa axis ticks number densities of our LBGs. Bottom panel shows the slope of a power law for the ACFs. Filled circles denote the slope for large-scale clustering ($40'' < \theta < 400''$; β_L) with no IC correction. Open circles indicate the slope for the all scales ($1'' < \theta < 1000''$) with IC correction, which correspond to results of the conventional power-law approximation presented in Table 1.

TABLE 1
SUMMARY OF CLUSTERING PROPERTIES

i'_{AB} (mag)	$N(< i')^{\text{a}}$	Conventional Power-Law Approximation				Model		
		$n(< i')^{\text{b}}$ (h_{70}^3 Mpc $^{-3}$)	A_{ω}^{c} (arcsec $^{\beta}$)	β^{c}	r_0^{c} (h_{100}^{-1} Mpc)	β_L^{d}	$\langle Ng \rangle$	$\log \langle M_h \rangle$ (h_{70}^{-1} M_{\odot})
24.5	239	$9.8 \pm 1.6 \times 10^{-5}$	25.3 ± 21.9	1.42 ± 0.55	$3.92^{+3.85}_{-3.92}$	$\simeq 0.99$	0.2	12.4
25.0	808	$2.8 \pm 0.3 \times 10^{-4}$	22.2 ± 14.9	1.31 ± 0.25	$4.61^{+1.74}_{-1.74}$	1.12 ± 0.46	0.5	12.3
25.5	2231	$6.4 \pm 0.6 \times 10^{-4}$	6.16 ± 3.43	1.07 ± 0.16	$4.27^{+0.81}_{-0.96}$	0.75 ± 0.48	0.6	12.0
26.0	4891	$1.3 \pm 0.1 \times 10^{-3}$	3.93 ± 1.14	0.93 ± 0.08	$4.68^{+0.50}_{-0.53}$	0.97 ± 0.18	0.6	11.9
26.5	8639	$2.2 \pm 0.3 \times 10^{-3}$	1.53 ± 0.38	0.73 ± 0.07	$4.51^{+0.28}_{-0.30}$	0.83 ± 0.13	0.7	11.8
27.0	12921	$3.7 \pm 0.7 \times 10^{-3}$	1.01 ± 0.20	0.65 ± 0.05	$4.28^{+0.19}_{-0.19}$	0.63 ± 0.08	0.7	11.8
27.5	16920	$5.8 \pm 1.4 \times 10^{-3}$	0.76 ± 0.15	0.62 ± 0.05	$3.87^{+0.13}_{-0.16}$	0.60 ± 0.08	0.7	11.7

^aCumulative numbers. Differential surface densities are 0.002 ± 0.001 , 0.014 ± 0.002 , 0.049 ± 0.004 , 0.158 ± 0.007 , 0.395 ± 0.011 , 0.739 ± 0.014 , 1.041 ± 0.017 , 1.189 ± 0.018 , 1.111 ± 0.018 , and 0.724 ± 0.014 arcmin $^{-2}$ (0.5mag) $^{-1}$ for $i' = 23.25$, 23.75 , 24.25 , 24.75 , 25.25 , 25.75 , 26.25 , 26.75 , 27.25 , and 27.75 , respectively, which are consistent with those of previous measurements (e.g. Ouchi et al. 2004a).

^bCumulative number density calculated from luminosity function of Giavalisco (2005).

^cResults from the conventional power-law approximation, i.e. $\omega(\theta) = A_{\omega}(\theta^{-\beta} - IC/A_{\omega})$, over $1'' - 1000''$. For integral constraints, IC, we apply $IC/A_{\omega} = [5, 10, 48, 123, 493, 868, 1070] \times 10^{-5}$ for $i' = [24.5, 25.0, 25.5, 26.0, 26.5, 27.0, 27.5]$.

^dPower-law slope for the fit of $\omega = A_{\omega}\theta^{-\beta}$ over $40'' - 400''$ which corresponds to $1 - 10h_{100}^{-1}$ Mpc. No IC correction is applied to β_L .